arXiv:1311.1145v1 [astro-ph.EP] 5 Nov 2013

Not to appear in Nonlearned J., 45.

Characterizing the purple Earth: Modelling the globally-integrated spectral variability of the Archean Earth

E. Sanromá[1,2], E. Pallé[1,2], M. N. Parenteau[3,4], N. Y. Kiang[5], A. M. Gutiérrez-Navarro[6], R. López[1,2] and P. Montañés-Rodríguez[1,2]

Instituto de Astrofísica de Canarias (IAC), Vía Láctea s/n 38200, La Laguna, Spain

mesr@iac.es

ABSTRACT

The ongoing searches for exoplanetary systems have revealed a wealth of planets with diverse physical properties. Planets even smaller than the Earth have already been detected, and the efforts of future missions are placed on the discovery, and perhaps characterization, of small rocky exoplanets within the habitable zone of their stars. Clearly what we know about our planet will be our guideline for the characterization of such planets. But the Earth has been inhabited for at least 3.8 Ga, and its appearance has changed with time. Here, we have studied the Earth during the Archean eon, 3.0 Ga ago. At that time one of the more widespread life forms on the planet were purple bacteria. These bacteria are photosynthetic microorganisms and can inhabit both aquatic and terrestrial environments. Here, we used a radiative transfer model to simulate the visible and near-IR radiation reflected by our planet, taking into account several scenarios regarding the possible distribution of purple bacteria over continents and oceans. We find that purple bacteria have a reflectance spectrum which has a strong reflectivity increase, similar to the red edge of leafy plants, although shifted redwards. This feature produces a detectable signal in the disk-averaged

[2]Departamento de Astrofísica, Universidad de La Laguna, Spain

[3]NASA Ames Research Center, Exobiology Branch, Mountain View, California 94035, USA

[4]SETI Institute, Mountain View, California 94035, USA

[5]NASA Goddard Institute for Space Studies, New York, NY 10025, USA

[6]Department of Microbiology, Faculty of Biology, University of La Laguna, Spain

spectra of our planet, depending on cloud amount and on purple bacteria concentration/distribution. We conclude that by using multi-color photometric observations, it is possible to distinguish between an Archean Earth in which purple bacteria inhabit vast extensions of the planet, and a present-day Earth with continents covered by deserts, vegetation or microbial mats.

Subject headings: Astrobiology — Earth — Planets and satellites: atmospheres, surfaces — Radiative transfer

1. INTRODUCTION

Since the discovery of the first exoplanet orbiting a main sequence star in 1995 (Mayor & Queloz 1995), nearly 950 extrasolar planets have been detected, and more than 2000 potential planet candidates from the Kepler mission are waiting to be confirmed (Batalha et al. 2013). In the last few years, we have been able to discover several planets in the super-Earth mass range (e.g. Udry et al. 2007; Charbonneau et al. 2009; Pepe et al. 2011; Borucki et al. 2012), some of them lying within, or close to, the habitable zone of their stars (e.g. Borucki et al. 2012; Barclay et al. 2013; Anglada-Escudé et al. 2013). Even some Earth and Moon-sized planets have been recently announced (Fressin et al. 2012; Muirhead et al. 2012; Gilliland et al. 2013; Borucki et al. 2013), and this number is expected to increase in the future. In fact, early statistics have pointed out that around 62% of the Milky Way's stars might host a super-Earth (Cassan et al. 2012), while studies from NASA's Kepler mission indicate that about 16.5% of stars have at least one Earth-size planet with orbital periods up to 85 days (Fressin et al. 2013). To be prepared for the characterization of future discovered exoearths, first we must take a look to our own solar system and its planets.

Without a doubt, the possibility of finding life will drive the characterization of rocky exoplanets over the coming decades. Earth is the only planet where life is known to exist; thus observations of our planet will be a key instrument for characterization and the search for life elsewhere. However, even if we discovered a second Earth, it is very unlikely that it would present a stage of evolution similar to the present-day Earth. The Earth has been far from static since its formation about 4.5 Ga ago. On the contrary, during this time, it has undergone multiple changes in its atmospheric composition, its temperature structure, its continental distribution, and even changes in the forms of life that inhabit it. All these changes have affected the global properties of Earth as seen from an astronomical distance. Thus, it is of interest not only to characterize the observables of the Earth as it is today, but also at different epochs (Kaltenegger et al. 2007; Sanromá & Pallé 2012).

Aiming at determining how Earth would look like to a hypothetical distant observer, several studies have been carried out over the last years. Earthshine observations have been one of the observational approaches used for this purpose, providing a tool to study the spectrum of Earth in the visible (e.g. Goode et al. 2001; Woolf et al. 2002; Qiu et al. 2003; Pallé et al. 2003, 2004), and also in the near-infrared (Turnbull et al. 2006; Pallé et al. 2009) and in the near-UV (Hamdani et al. 2006). Sterzik et al. (2012) studied the use of the linear polarization content of the earthshine to detect clouds and biosignatures.

Another possible approach is through analysis of Earth's observations obtained from remote-sensing platforms (e.g., Tinetti et al. 2006a; Cowan et al. 2011; Robinson et al. 2011; Fujii et al. 2013). Cowan et al. (2009) performed principal components analysis in order to determine if it was possible to identify surface features such as oceans and continents from the EPOXI data. They were able to reconstruct a longitudinally averaged map of the Earth' surface. Crow et al. (2011) were able to categorize Earth among the planets of the solar system by using visible colors.

Also using EPOXI data, Kawahara & Fujii (2010, 2011) and Fujii & Kawahara (2012) proposed an inversion technique which allowed them to sketch two-dimensional planetary albedo maps from annual variations of the disk-integrated scattered light.

Some authors have attempted to detect the vegetation red edge through earthshine measurements (Arnold et al. 2002; Woolf et al. 2002; Seager et al. 2005; Montañés-Rodríguez et al. 2006; Hamdani et al. 2006), and also using simulations (Tinetti et al. 2006a,b; Montañés-Rodríguez et al. 2006). The red edge is characterized by strong absorption in the visible part of the spectrum due to the presence of chlorophyll, which contrasts with a sharp increase in reflectance in the NIR due to scattering from the refractive index difference between cell walls and the surrounding media. This particular signature of vegetation has been proposed as a possible biomarker in Earth-like planets (e.g., Seager et al. 2005; Montañés-Rodríguez et al. 2006; Kiang et al. 2007a). The possibility of detecting hypothetical alien vegetation on terrestrial planets has also been studied. Tinetti et al. 2006c explored the detectability of exovegetation in a planet orbiting an M star, on which vegetation photosynthetic pigments might show a shifted red edge signature. Kiang et al. 2007b conjectured further about rules for pigments adaptations to other stellar types.

In this paper we concentrate on the Archean eon (3.8-2.5 Ga ago), particularly on the Earth at 3.0 Ga ago when the Sun was about 80% as bright as it is today (Gough 1981; Bahcall et al. 2001), and the atmospheric composition of our planet was completely different to that of present day. At this time, the Earth's atmosphere was likely dominated by N_2, CO_2, and water vapor (e.g., Walker 1977; Pinto et al. 1980; Kasting 1993; Kasting & Brown 1998), with little or no free oxygen. Methane might have also been present as well, help-

ing in the compensation for the reduced solar luminosity (e.g., Kiehl & Dickinson 1987; Pavlov et al. 2000; Haqq-Misra et al. 2008).

While controversial, the first evidence of life is at 3.8 Ga in isotopically light graphite inclusions in apatite from Greenland (Mojzsis et al. 1996), and most likely it was non-photosynthetic, although this is still a subject of debate. The earliest photosynthetic life was probably anoxygenic bacteria like purple bacteria (Xiong et al. 2000; Olson 2006), utilizing reductants such as H_2 or H_2S instead of water. The Archean biosphere has been proposed to be a mix of anoxygenic phototrophs and chemotrophs such as sulfate-reducing bacteria, methanogens, and other anaerobes (Kharecha et al. 2005). The former perform photosynthesis requiring a band gap energy smaller than that needed to split water, such that the photosynthetically active radiation relevant for anoxygenic photosynthetic bacteria can extend into the near-infrared to as long as ∼1025 nm (Scheer 2003). Thus, their color is distinctly different from that of land plants that dominate the Earth today.

Because directly imaged extrasolar planets are unlikely to be spatially-resolved, we will have all planet's information collapsed in a single point of light. Thus, disk-averaged views of Earth are one of the best way to understand what kind of information one can expect from such type of observations of an Earth analogue. In this paper, we present disk-integrated spectra of the ancient Earth, with the aim of discerning the effect that a different composition of the atmosphere, and the presence of purple bacteria in different land/ocean configurations, might have had in the way our planet looked from afar.

2. MODEL DESCRIPTION

For our calculations, we make use of a line-by-line radiative transfer algorithm, based on the DISORT[1] (Discrete Ordinates Radiative Transfer Program for a Multi-Layered Plane-Parallel Medium) code (Stammnes et al. 1988), in order to derive disk-integrated spectra of the early Earth. This radiative transfer model (RTM) utilizes spectral albedo of different surface types, profiles of atmospheric composition and temperature, cloudiness information, and viewing and illumination angles as input data for the calculations. Only a single angle of incidence and ten angles of reflection can be used for each model run. The RTM used here is basically an extension of the RTM for transits described in García Muñoz & Pallé (2011) and García Muñoz et al. (2012) to a viewing geometry for which the light reaching the observer has been reflected at the planet. With this RTM, we have generated a database of about 160 one-dimensional synthetic spectra that cover a wide range of illumination and

[1]ftp://climate1.gsfc.nasa.gov

viewing angles, and different surface and cloud types. Each spectrum has been calculated at very high spectral resolution, with at least three points per Doppler width, although, we have degraded them to a lower resolution (R= $10,000$) for storage purposes. Once the one-dimensional spectral library was constructed, we calculated the disk-averaged irradiance of the early Earth given a particular viewing/illumination geometry, and a map of surface properties, as described in Section 2 of Sanromá et al. (2013).

It is worth noting that, unlike in Sanromá et al. (2013) where clouds are prescribed through a semi-empirical model, for the Archean there is a complete lack of reliable information on cloudiness behavior. Thus we have assumed that the same cloud frequency occurs at each grid point, with this cloud amount an input parameter in our model.

2.1. Atmospheric Properties

Temperature and atmospheric composition profiles for the Archean were calculated by R. Ramirez (private communication). A 1-D radiative-convective climate model, first developed by Kasting et al. (1984) and recently substantially updated by Kopparapu et al. (2013) and Ramirez et al. (2013), was used to calculate the atmospheric properties.

These atmospheric profiles consist of 1% CO_2, 0.2% CH_4, according to Kaltenegger et al. (2007), being the remaining gas N_2. For the relative humidity, a Manabe-Wetherald profile was used (Manabe & Wetherald 1967). For the calculation of these profiles the Sun was assumed to have ∼79% of its present-day luminosity, as we aimed to simulate the Earth 3.0 Ga ago. The temperature and mixing ratios profiles of these species are shown in Figure 1.

In our model, we divided the atmosphere into 33 uneven layers, which go from the boundary layer to 100 Km height, with the spacing between layers of 1 km near the bottom of the atmosphere, and 5 km or more above 25 km height. As the original atmospheric profiles were prescribed in layers up to 70 Km, we assumed the same constant values between 70 and 100 Km.

2.2. Surface Properties

To perform the disk-averaged spectra of the ancient Earth, we have considered four different planetary surfaces: water, desert, water with purple bacteria in suspension, and purple bacteria in microbial mats. There is some discussion in the literature whether purple non-sulphur bacteria could have colonized extended areas of soil, and whether such a signal would be remotely detectable. Here we have assumed as the most likely scenario, that these

microbial mats are located in marine intertidal environments. The wavelength-dependent surface reflectivity of the two first surface types were derived from the ASTER Spectral Library[2] and the USGS Digital Spectral Library[3]. Figure 2 shows the spectral albedo of these surface types. The wavelength-dependent albedo of surfaces involving purple bacteria were obtained as described in Section 3 (Figure 3).

2.3. Surface Distribution

The movement of Earth's tectonic plates has caused the formation and the break up of continents over Earth's history, including the formation of supercontinents. The orientation of Earth's earliest continents is still unknown, although it is believed that the fraction of the surface covered by continents during the Archean was smaller than present day (e.g. Goodwin 1981; Belousova et al. 2010; Dhuime et al. 2012). Earth might have been almost entirely covered by water with some small continents. Hence, due to the complete lack of information about the continental distribution of the Earth 3.0 Ga ago, we decided to use that of the Earth during the Late Cambrian (500Ma ago, see Figure 4) and at present day, as two possible characteristics examples. The continental distribution of these two epochs has been taken from Ron Blakey's website[4], where these surface maps are available online. The Earth geologic information has been regridded into the 64x32 pixel grid used by our model.

We have also defined the coastal areas of these maps. These coastal zones were determined as those land grid cells that have adjacent ocean grid cells and those ocean cells that have adjacent land grid cells.

2.4. Cloud Optical Properties

For these simulations we have taken into account three different cloud layers: low (1000-680 mb), mid (680-440 mb) and high cloud (440-30 mb). The optical properties of each cloud type, wavelength-dependent scattering and absorption coefficients, and the asymmetry parameter, were taken from the Optical Properties of Aerosols and Clouds (OPAC) data base (Hess et al. 1998). We have considered physical cloud thicknesses of 1 km, and we have

[2]http://speclib.jpl.nasa.gov

[3]http://speclab.cr.usgs.gov/spectral-lib.html

[4]http://jan.ucc.nau.edu

assumed that the scattering phase function is described by the Henyey-Greenstein equation inside clouds, and by the Rayleigh scattering function outside them.

The atmospheric composition of our planet has not changed drastically in the last 500 Ma. On average, the same atmospheric composition and mean averaged temperature have existed during this period (Hart 1978; Kasting & Siefert 2002). Hence, in Sanromá et al. (2013) we used a semi-empirical model of clouds in order to reconstruct the possible cloud distribution of the Earth in the past, up to 500 Ma ago. However, this does not hold true for longer period of time, and such cloudiness reconstruction is not a valid approximation for the Archean. Thus, we prescribe the mean cloud frequency of the Archean as an input parameter, and explore how different levels of cloudiness may have affected the way our planet looked from afar, and in particular, the effect that could have had in the possible detection of biomarkers. Note that detailed cloud structures, tied to ocean currents or continents, are missing in or simulations. However, for globally-integrated spectra like the ones investigated here, this limitation is small.

3. PURPLE BACTERIA'S REFLECTANCE SPECTRA

To obtain the reflectance spectra of purple bacteria, we used pure cultures of *Rhodobacter sphaeroides* ATCC 49419, a purple non-sulfur bacterium growing as a suspension of cells in liquid media. This type of phototroph exhibits diverse metabolic abilities, allowing survival in a wide range of dynamic environmental conditions. Purple non-sulfurs can grow aerobically in the dark as a chemoheterotroph, and anaerobically in the light using hydrogen and organic compounds as electron donors for photosynthesis.

We made two different measurements to retrieve the reflectance spectrum of these bacteria. In the first one, the reflectance of a liquid pure culture of purple bacteria was measured using a UV/VIS/NIR spectrophotometer (VARIAN, CARY 5E). The measurements were taken from 0.3 to 2.5 μm.

In the second experiment, we used a LiCor LI1800 spectroradiometer with a remote cosine receptor that was positioned 5 cm above the culture. These measurements cover the 0.35-1.1 μm spectral range. This culture of purple bacteria was in a petri dish sitting on top of a piece of white paper. In order to calculate the spectral albedo, the spectral irradiance of the Sun was also measured.

Both sets of retrieved reflectances spectra were merged into one, covering from the visible to the near-infrared (Figure 3), using as a reference the second experiment, which had a higher signal to noise ratio. In order to absolutely calibrate the reflectance spectra

of the bacteria, we also measured the reflectance spectra of a set of known leaves. The comparison of our measured leaf reflectance spectra with those tabulated in the ASTER library gave us a measure of our reflected flux, which we then applied to the reflectance spectra of the purple bacteria. This way we transformed the ratio scale into a reflectance scale.

Figure 3 shows the reflectance spectrum of the purple non-sulfur bacterium *Rhodobacter sphaeroides*. The photosynthetic pigments of these bacteria are *bacteriochlorophyll a* esterified with phytol, and carotenoids of the spirilloxanthin series. Due to the combination of these two pigments, living cells of this species show absorption features at 375, 468, 493, 520-545, 589, 802, 860-875 nm (Imhoff 2005). Some of these features can be detected, and are marked, in Figure 3. Moreover, as the purple non-sulfur bacteria cultures used were red, the reflectance increase between ∼600 and 700 nm is due to the reddish light reflected back from the cultures' cells. The most noticeable feature of this spectrum is the sharp increase in reflectivity from approximately 0.9 μm to 1.1 μm, and the equally strong decrease from 1.3 μm to 1.4 μm. Information about the physical nature of the absorption features at $\lambda >$ 1 μm is not found in the literature. Starting at 1.4 μm and redwards, the spectrum does not show any measurable features, and the overall albedo value is probably that of water, made slightly more reflective due to the presence of bacteria in suspension that lower its transmissivity. The overly-featureless variability is probably due to the low sensitivity of the instrument used at these wavelengths.

The bacteria concentration in our sample culture was very high (∼10^9 cells/ml), probably much more than the typical concentrations that would be found in seawater. Thus, when we modeled purple bacteria in open oceans, we used a combination of pure seawater and our bacteria(+water) spectra, weighted in varying percentages, to simulate different bacteria concentrations. Throughout the rest of the paper we refer to percentage dissolution (for example a dissolution of 10% means 9 parts of seawater and 1 part of our culture, equivalent to concentrations of the order of ∼10^8 cells/ml). Note that as we used liquid cultures to measure the reflectance of purple bacteria, the effect of the transmittance of water is already included in the spectrum.

4. THE SPECTRA OF THE EARLY EARTH

In order to determine if it would be possible to discern the presence of life forms such as purple bacteria in the spectra of an extrasolar planet, we have simulated the disk-integrated spectra of the ancient Earth, taking into account different continental distribution, cloud coverage, and several abundance scenarios which go from a planet where purple bacteria

have colonized both oceans and continents, to a planet where purple bacteria are only found in oceanic coastal areas in low concentrations.

In all the cases studied in this manuscript, both the observer and the Sun are located over the planet's equator in such a way that the observer is looking at a half-illuminated planetary disk, i.e., at a phase angle of 90°. This is the most relevant geometry for studying exoplanets, since the maximum angular separation of an extrasolar planet from its parent star along its orbit, takes place at phase 90°, as defined from the observer's position.

In order to see the effect of considering different atmospheric compositions in the disk-averaged spectra of a lifeless planet, Figure 5 compares the spectrum of a planet with a CO_2-CH_4 rich atmosphere and no oxygen (black), with the spectrum of a planet with Earth's current atmospheric composition (blue). In both cases, the continental distribution is that of Earth 500 Ma ago and continents are assumed to be completely covered by deserts. Figure 5 (black lines) show strong absorption in the NIR part of the spectrum due to the increased levels of CO_2 and CH_4, while in the visible region, the most noticeable difference with Earth's current atmosphere is the lack of the absorption features typical of O_2 and O_3.

4.1. The effects of clouds

The visibility of surface inhomogeneities, such as continents or surface types, on a planet is naturally very dependent on the frequency of cloud formation. The top panels of Figure 6 shows synthetic disk-averaged spectra of the ancient Earth over a course of a day, one spectrum every two hours, covering the spectral range between 0.4 and 2.5 μm, for both a cloud free (left) and a cloudy atmosphere (right). Cloud cover is assumed to be 50%. In the top panels, the continental distribution corresponds to that of Earth 500Ma ago, and continents are dry lands (deserts), while the coastal points closest to land are completely covered by purple bacteria, and the coastal points closest to ocean are a mixture of 10% purple bacteria and 90% of water. We have chosen this particular scenario since bacteria are expected to be found where nutrients are more abundant, like in shallow waters or coastal zones.

It is expected that as continents come in and out of the field of view, the light reflected back by the Earth changes, with these changes more drastic for the cloud-free cases. The reflectance is higher when continents occupy most of the observable half-disk (at 8:00-10:00 UT, when the percentage of continental surface in the sunlit area of the planet visible from our observer's location is ∼50%), than when oceans dominate the field of view (at 16:00-18:00 UT, when the percentage of continental surface is ∼95%).

The addition of clouds to the model results in a overall enhancement of the light reflected back by the planet, and a strong decrease in the reflectance variability over a diurnal cycle. This results in a significant loss of information about the surface types lying under clouds. It is worth noting that changing cloud cover or even varying cloudiness distribution could significantly change the overall shape of these disk-averaged spectra.

4.2. The effects of continental distribution

The land-mass distribution of the Earth 500 Ma ago consisted of a large continental mass, mostly located in the southern hemisphere. There is also a further group of three large islands also in the southern hemisphere. On the other hand, the present-day Earth has two major continental land masses spreading over the north and southern hemispheres. In order to estimate the effect of considering different land-mass distributions, Figure 6 bottom panels show the same spectra as the top panels, but here the input continental distribution corresponds to that of the present-day Earth. Although these two continental distributions are considerably different, the disk-integrated spectra of both cases are quite similar. The rotational variability is also similar in both cases, with a comparable amplitude, only slightly smaller for the present day Earth when clouds are considered.

4.3. Abundances and detectability

Figure 7 (left) shows disk-integrated spectra obtained for the early Earth where continents are completely covered by purple bacterial mats, and oceans are a mixture of water and bacteria, 90% and 10%, respectively. Both a cloud-free (red) and a 50% cloudy case (black) are shown. The continental distribution used here is that of Earth 500Ma ago.

Whether purple bacteria would have been able to colonize the continental surfaces during the Achean is still unsolved. Due to the lack of O_2 in the early Earth's atmosphere, and therefore the lack of a ozone layer, harmful radiation did probably reach the Earth's surface, and purple bacteria might have suffered from DNA damage. Studies of modern microbes, however, suggest that their photoprotective pigments, that absorb in the blue and UV (e.g., carotenoids), are sufficient to have allowed for their survival in terrestrial and shallow water environments on the early Earth (Cockell 1998). Moreover, some purple bacteria have been shown to use reduced iron (Fe(II)) for photosynthesis, and Pierson et al. (1993) pointed out that the oxidized iron products of this type of photosynthesis could have provided substantial protection from UV radiation for surface-dwelling phototrophs prior to the development of

an ozone shield. Thus, the presence of bacterial mats in continental areas, while not being our most likely scenario, cannot be ruled out.

In Figure 7 (left) we only show the spectra at the time when the continental presence is at maximum, i.e., at 08:00 UT, when the percentage of land over ocean that is illuminated and visible at the same time is about 50%. The same is shown in the right panel of this Figure, but here considering that purple bacteria do not exist over continents, and are only found in the oceans. For comparison, Figure 5 (black lines) shows the spectra of a planet without bacteria in either water or land.

When the amount of purple bacteria is high, 100% over continents and 10% diluted in the water, the presence of purple bacteria on the early Earth produces a strong feature, a steep increase in reflectance around 1.0 μm in its disk-integrated spectrum (Figure 7 left). When clouds are included in the model, this signature is naturally significantly diluted. However, it is still easily detectable by simple inspection of the disk-average spectra.

When considering a more realistic case where purple bacteria are only found in coastal areas (Figure 6), the increase in reflectivity around 1.0 μm due to these bacteria is readily seen in the cloud-free case and is still detectable in the cloudy case.

For a planet with marine bacterial life only, and bare continental surfaces, this spectral feature produced by purple bacteria becomes harder to discriminate in the spectra (Figure 7 right), being practically undetectable in the cloudy case. Here we have considered a mixture of 10% bacteria and 90% water. In fact, if one compares the cloudy spectrum of this case with a case where there are no bacteria, neither over continents nor in the water (Figure 5, black lines) it is impossible to distinguish between them by simple exploration of the spectra. Thus, to estimate the marine-only purple bacteria detectability, we have considered several bacteria concentrations in oceans: 20, 30, 40, and 50%. Table 1 shows the slope of the straight line that connects the averaged planetary radiance in the 0.745-0.770 μm and 1.010-1.034 μm spectral intervals. The data are given as a function of bacteria concentration in water for both a cloud-free and a cloudy atmosphere. The slope between these two spectral regions, free of atmospheric absorption features, is mainly influenced by the contribution of purple bacteria to the globally-integrated spectrum of Earth. Thus, this slope can be used as a measure of the strength of the purple bacteria signal, similar to what has been previously done with to quantify the vegetation's red edge (Montañés-Rodríguez et al. 2006). Table 1 shows how increasing the bacteria concentration in water from 10% to 50% monotically increases this slope. Although not shown here, the identification of the presence of purple bacteria by simple inspection of these spectra in the cloudy atmosphere case is almost impossible for bacteria concentrations in oceans lower than 30%.

Finally, although it is a very improbable scenario, we have run a comparison test to estimate the purple bacteria detectability. Figure 8 shows disk-averaged spectra of Earth considering the present-day continental and cloud distribution, and the early Earth atmosphere. Cloud distribution was taken as the 1984-2006 climatology of ISCCP[5] cloudiness data. Here we have assumed that continents are completely deserts and we have used the 2012 annual mean ocean chlorophyll a content map from the SeaWiFS project[6] as a proxy for the distribution of purple bacteria. Thus, we have considered that the ocean latitudinal range 90°—35°, both Nord and South, and the -10°—10°latitudinal range are a mixture of 90% bacteria and 10% of water. Coastal zones are also populated with purple bacteria, and the rest of the ocean is a mixture of 10% bacteria and 90% water. The figure shows the spectra at 8:00 UT (when oceans dominate the field of view; blue lines) and at 18:00 UT (when continents dominate the field of view; black lines). As in previous cases in a cloud-free atmosphere purple bacteria are readily detectable. For a present-day cloud amount (roughly 60%) the detectability is not so obvious, and a high signal-to-noise ratio spectra of the planet would be needed.

5. Photometric Light-Curves

In the case of a terrestrial planet in the habitable zone of a G, F or K star, obtaining in the near-future even a low resolution spectra might be a difficult task to perform (e.g., Pallé et al. 2011; Rugheimer et al. 2013; Hedelt et al. 2013). Photometric observations on a few filters might actually be a more realistic possibility, even if the data are obtained via spectroscopic observations, as is the case of Hubble and Spitzer observations nowadays (e.g., Tinetti et al. 2007; Swain et al. 2008; Désert et al. 2011; Pont et al. 2013). The fact that a planet shows photometric variability along one rotation already speaks about the presence of inhomogeneities in its surface or atmosphere (Ford et al. 2001). With sufficiently accurate time series it might be possible to distinguish the presence of cloudiness and continents based on this variability (Pallé et al. 2008). Moreover, the rotational photometric variability as a function of wavelength can reveal information about the major wide-spread composition of continental surfaces.

Thus, following Sanromá et al. (2013), we have convolved our modeled disk-integrated spectra against standard astronomical filters, both visible and near-infrared, namely B, V, R, I, z, J, H, and K. Figure 9 shows the photometric daily variations in each photometric

[5]http://isccp.giss.nasa.gov

[6]http://oceancolor.gsfc.nasa.gov/

filter of the disk-averaged reflected light, for a cloud-free atmosphere (red) and for a cloudy one (black).

For these simulations, we have used a conservative scenario: the continental distribution assumed is that of Earth 500 Ma ago, continents are bare desert, coastal land areas are covered by purple bacteria mats, oceanic coastal areas are a mixture of 10% purple bacteria and 90% of water, and open ocean areas are only water.

The light curves shown in Figure 9 all have a similar shape; the peak in brightness takes place in each of the photometric filters when continents dominate the field of view, between 8:00 and 10:00 UT, while minimum values of reflectance occur when oceans occupy most of the view, approximately at 4:00 and at 16:00 UT.

The cloud-free case shows a larger variability in the diurnal light curves in each filter and a considerable rise in brightness that increases monotically redwards. A similar result is found when clouds are added to the model, although it shows much less variability owing to the effect of clouds on the spectra.

Figure 10 (top) shows the amplitude of albedo variations of the two scenarios shown in Figure 9 as a function of the different photometric filters. As found before, the variability of the light reflected back by the planet in both the cloud-free and cloudy cases increases toward the red, with this increase much more dramatic in the cloud-free case than in the cloudy one. The amplitude of these variations goes from a few percents to around 180% and 50%, for a cloud-free and a cloudy atmosphere, respectively.

Figure 10 (bottom) shows the expected photometric variability for a modern Earth with different surface compositions (data from Sanromá et al. 2013), together with the Archean Earth results for the cloudy case (from top panel). The different color lines show the amplitude of the albedo variability for a cloudy atmosphere with an atmospheric composition similar to that of present Earth, for a planet totally desert (black line), completely covered by vegetation (green line), by microbial mats (red and dark blue lines), and for a planet where continents are a mixture of microbial mats and deserts (yellow line), and microbial mats and vegetation (cyan line). In all cases the atmospheric composition in the models used to generate the data is that of the modern Earth. The purple line shows the albedo variability of a cloudy planet with an atmospheric composition similar to that of the early Earth (3.0 Ga ago) which continents are covered by deserts and coasts are a mixture of purple bacteria and water.

In Sanromá et al. (2013) we concluded that it would be possible to discriminate between vegetated continents, large extension of microbial mats and bare continental surfaces by comparing the amplitude of the albedo change, along the course of a day, taken in different

photometric filters. Here, the purple curve suggests that it would also be possible to discriminate a purple Archean-like planet among the other scenarios studied in Sanromá et al. (2013). In contrast to the other scenarios, in the visible portion of the spectrum, the amplitude of albedo change of the Archean Earth increases monotically from the B filter to the z filter, an effect due to the combination of the lack of oxygen in the atmosphere and the reflectance spectra of the purple bacteria. When one moves towards the red part of the spectrum, this increase is sharper and the curve peaks at the H filter to decrease redwards in K. However, if one only takes into account the near-IR filters, it would be difficult to discriminate between a desert planet and the purple scenario.

6. CONCLUSIONS

In this paper we have presented disk-integrated spectra of the Earth during the Archean eon with the aim of studying how a different atmospheric composition and the presence of early life forms, such as purple bacteria, may have affected the way our planet looked from afar.

As one of the inputs of our models is the reflectance spectrum of different surface types, we carried out two different experiments in order to retrieve the spectral albedo of these bacteria in the spectral rage 0.3-2.5 μm. We found that purple bacteria show a reflectance spectrum with a sharp increase in reflectivity similar to the red edge of leafy plants, but shifted redwards.

In order to determine if it would be possible to detect such a biomarker, we have considered three different scenarios: one where purple bacteria have colonized the whole planet, both water and continents, other where purple bacteria are only found in oceans, and finally a scenario where these bacteria are found only in coastal regions. We have taken into account the effect of clouds in our models finding that the inclusion of clouds results in the increase of the reflectivity of the planet, reduces drastically the albedo variability over the course of a day, and makes more difficult the identification of surface types under clouds. Changing the continental distribution does not seem to have a high impact in the globally-averaged spectral variations.

We find that when the amount of purple bacteria is high, they can be readily detected in disk-averaged spectra, both in cloud-free and in cloudy atmospheres. While if purple bacteria are only found in oceans, their spectral feature becomes nearly undetectable in the cloudy case. When considering a more realistic scenario where purple bacteria are found in coasts, their presence can be detectable in the cloud-free case, and even in the cloudy case,

although the signal is smaller.

Finally, by convolving these simulated spectra against standard astronomical filters, we conclude that using photometric observations in different filters might allow us to discriminate between a present day Earth with continental surface covered by deserts, vegetation or microbial mats, from an Archean Earth where purple bacteria have colonized large extensions of the planet.

Acknowledgments

We would like to thank Antígona Segura and Ramses Ramirez for kindly providing us with the atmospheric profiles of the early Earth.

REFERENCES

Anglada-Escudé, G., Tuomi, M., Gerlach, E., et al. 2013, A&A, 556, A126

Arnold, L., Gillet, S., Lardière, O., Riaud, P., & Schneider, J. 2002, A&A, 392, 231

Bahcall, J. N., Pinsonneault, M. H., & Basu, S. 2001, ApJ, 555, 990

Barclay, T., Burke, C. J., Howell, S. B., et al. 2013, ApJ, 768, 101

Batalha, N. M., Rowe, J. F., Bryson, S. T., et al. 2013, ApJS, 204, 24

Belousova, E. A., Kostitsyn, Y. A., Griffin, W. L., et al. 2010, Lithos, 119, 457

Borucki, W. J., Agol, E., Fressin, F., et al. 2013, Science, 340, 587

Borucki, W. J., Koch, D. G., Batalha, N., et al. 2012, ApJ, 745, 120

Cassan, A., Kubas, D., Beaulieu, J.-P., et al. 2012, Nature, 481, 167

Charbonneau, D., Berta, Z. K., Irwin, J., et al. 2009, Nature, 462, 891

Cockell, C. S. 1998, J Theor Biol, 193, 717

Cowan, N. B., Agol, E., Meadows, V. S., et al. 2009, ApJ, 700, 915

Cowan, N. B., Robinson, T., Livengood, T. A., et al. 2011, ApJ, 731, 76

Crow, C. A., McFadden, L. A., Robinson, T., et al. 2011, ApJ, 729, 130

Désert, J.-M., Bean, J., Miller-Ricci Kempton, E., et al. 2011, ApJ, 731, L40

Dhuime, B., Hawkesworth, C. J., Cawood, P. A., & Storey, C. D. 2012, Science, 335, 1334

Ford, E. B., Seager, S., & Turner, E. L. 2001, Nature, 412, 885

Fressin, F., Torres, G., Charbonneau, D., et al. 2013, ApJ, 766, 81

Fressin, F., Torres, G., Rowe, J. F., et al. 2012, Nature, 482, 195

Fujii, Y. & Kawahara, H. 2012, ApJ, 755, 101

Fujii, Y., Turner, E. L., & Suto, Y. 2013, ApJ, 765, 76

García Muñoz, A. & Pallé, E. 2011, J. Quant. Spec. Radiat. Transf., 112, 1609

García Muñoz, A., Zapatero Osorio, M. R., Barrena, R., et al. 2012, ApJ, 755, 103

Gilliland, R. L., Marcy, G. W., Rowe, J. F., et al. 2013, ApJ, 766, 40

Goode, P. R., Qiu, J., Yurchyshyn, V., et al. 2001, Geophys. Res. Lett., 28, 1671

Goodwin, A. M. 1981, Science, 213, 55

Gough, D. O. 1981, Sol. Phys., 74, 21

Hamdani, S., Arnold, L., Foellmi, C., et al. 2006, A&A, 460, 617

Haqq-Misra, J. D., Domagal-Goldman, S. D., Kasting, P. J., & Kasting, J. F. 2008, Astrobiology, 8, 1127

Hart, M. H. 1978, Icarus, 33, 23

Hedelt, P., von Paris, P., Godolt, M., et al. 2013, A&A, 553, A9

Hess, M., Koepke, P., & Schult, I. 1998, Bull. Am. Met. Soc., 79, 831

Imhoff, J. 2005, Genus IX. Rhodopseudomonas. In: Bergey's Manual of Systematic Bacteriology, vol 2, 2nd Edition (Brenner, DJ., Krieg, N.R. Staley, J.T., Springer. New York)

Kaltenegger, L., Traub, W. A., & Jucks, K. W. 2007, ApJ, 658, 598

Kasting, J. F. 1993, Science, 259, 920

Kasting, J. F. & Brown, L. L. 1998, The early atmosphere as a source of biogenic compounds. In the molecular origin of life

Kasting, J. F., Pollack, J. B., & Ackerman, T. P. 1984, Icarus, 57, 335

Kasting, J. F. & Siefert, J. L. 2002, Science, 296, 1066

Kawahara, H. & Fujii, Y. 2010, ApJ, 720, 1333

Kawahara, H. & Fujii, Y. 2011, ApJ, 739, L62

Kharecha, P., J., K., & Siefert, J. 2005, Geobiology, 3, 53

Kiang, N. Y., Segura, A., Tinetti, G., et al. 2007a, Astrobiology, 7, 252

Kiang, N. Y., Siefert, J., Govindjee, & Blankenship, R. E. 2007b, Astrobiology, 7, 222

Kiehl, J. T. & Dickinson, R. E. 1987, J. Geophys. Res., 92, 2991

Kopparapu, R. K., Ramirez, R., Kasting, J. F., et al. 2013, ApJ, 765, 131

Manabe, S. & Wetherald, R. T. 1967, Journal of Atmospheric Sciences, 24, 241

Mayor, M. & Queloz, D. 1995, Nature, 378, 355

Mojzsis, S. J., Arrhenius, G., McKeegan, K. D., et al. 1996, Nature, 384, 55

Montañés-Rodríguez, P., Pallé, E., Goode, P. R., & Martín-Torres, F. J. 2006, ApJ, 651, 544

Muirhead, P. S., Johnson, J. A., Apps, K., et al. 2012, ApJ, 747, 144

Olson, J. 2006, Photosynth Res, 88, 109

Pallé, E., Ford, E. B., Seager, S., Montañés-Rodríguez, P., & Vazquez, M. 2008, ApJ, 676, 1319

Pallé, E., Goode, P. R., Montañés-Rodríguez, P., & Koonin, S. E. 2004, Science, 304, 1299

Pallé, E., Goode, P. R., Yurchyshyn, V., et al. 2003, J. Geophys. Res. (Atmos.), 108, 4710

Pallé, E., Zapatero Osorio, M. R., Barrena, R., Montañés-Rodríguez, P., & Martín, E. L. 2009, Nature, 459, 814

Pallé, E., Zapatero Osorio, M. R., & García Muñoz, A. 2011, ApJ, 728, 19

Pavlov, A. A., Kasting, J. F., Brown, L. L., Rages, K. A., & Freedman, R. 2000, J. Geophys. Res., 105, 11981

Pepe, F., Lovis, C., Ségransan, D., et al. 2011, A&A, 534, A58

Pierson, B. K., Mitchell, H. K., & Ruff-Roberts, A. L. 1993, Origins of Life and Evolution of the Biosphere, 23, 243

Pinto, J. P., Gladstone, G. R., & Yung, Y. L. 1980, Science, 210, 183

Pont, F., Sing, D. K., Gibson, N. P., et al. 2013, MNRAS, 432, 2917

Qiu, J., Goode, P. R., Pallé, E., et al. 2003, J. Geophys. Res. (Atmos.), 108, 4709

Ramirez, R., Kopparapu, R., Zugger, M. E., et al. 2013, Nat.Geosc. (in review)

Robinson, T. D., Meadows, V. S., Crisp, D., et al. 2011, Astrobiology, 11, 393

Rugheimer, S., Kaltenegger, L., Zsom, A., Segura, A., & Sasselov, D. 2013, Astrobiology, 13, 251

Sanromá, E. & Pallé, E. 2012, ApJ, 744, 188

Sanromá, E., Pallé, E., & García Munõz, A. 2013, ApJ, 766, 133

Scheer, H. 2003, The pigments. In Advances in Photosynthesis and Respiration, Vol. 13: Light-Harvesting Antennas in Photosynthesis (B.R. Green and W.W. Parson, Dordrecht, The Netherlands, Kluwer Academic Publishers, pp. 29-81)

Seager, S., Turner, E. L., Schafer, J., & Ford, E. B. 2005, Astrobiology, 5, 372

Stammnes, K., Tsay, S. C., Wiscombre, W., & Jayaweera, K. 1988, Appl. Opt., 27, 2502

Sterzik, M. F., Bagnulo, S., & Palle, E. 2012, Nature, 483, 64

Swain, M. R., Vasisht, G., & Tinetti, G. 2008, Nature, 452, 329

Tinetti, G., Meadows, V. S., Crisp, D., et al. 2006a, Astrobiology, 6, 34

Tinetti, G., Meadows, V. S., Crisp, D., et al. 2006b, Astrobiology, 6, 881

Tinetti, G., Rashby, S., & Yung, Y. L. 2006c, ApJ, 644, L129

Tinetti, G., Vidal-Madjar, A., Liang, M.-C., et al. 2007, Nature, 448, 169

Turnbull, M. C., Traub, W. A., Jucks, K. W., et al. 2006, ApJ, 644, 551

Udry, S., Bonfils, X., Delfosse, X., et al. 2007, A&A, 469, L43

Walker, J. C. G. 1977, Evolution of the atmosphere

Woolf, N. J., Smith, P. S., Traub, W. A., & Jucks, K. W. 2002, ApJ, 574, 430

Xiong, J., Fischer, W., Inoue, K., Nakahara, M., & Bauer, C. 2000, Science, 289, 1724

This preprint was prepared with the AAS LaTeX macros v5.2.

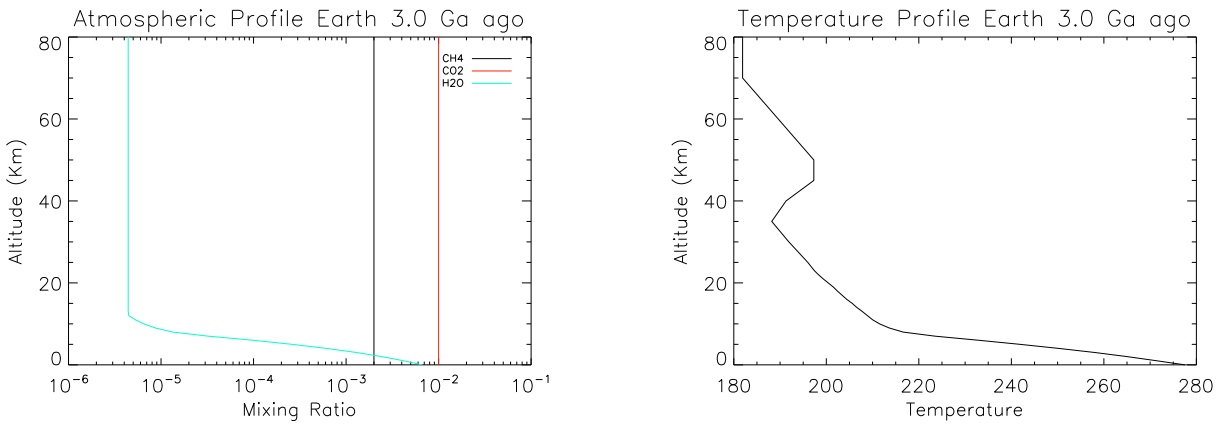


Fig. 1.— Atmospheric composition and temperature profiles of the Earth 3.0 Ga ago.

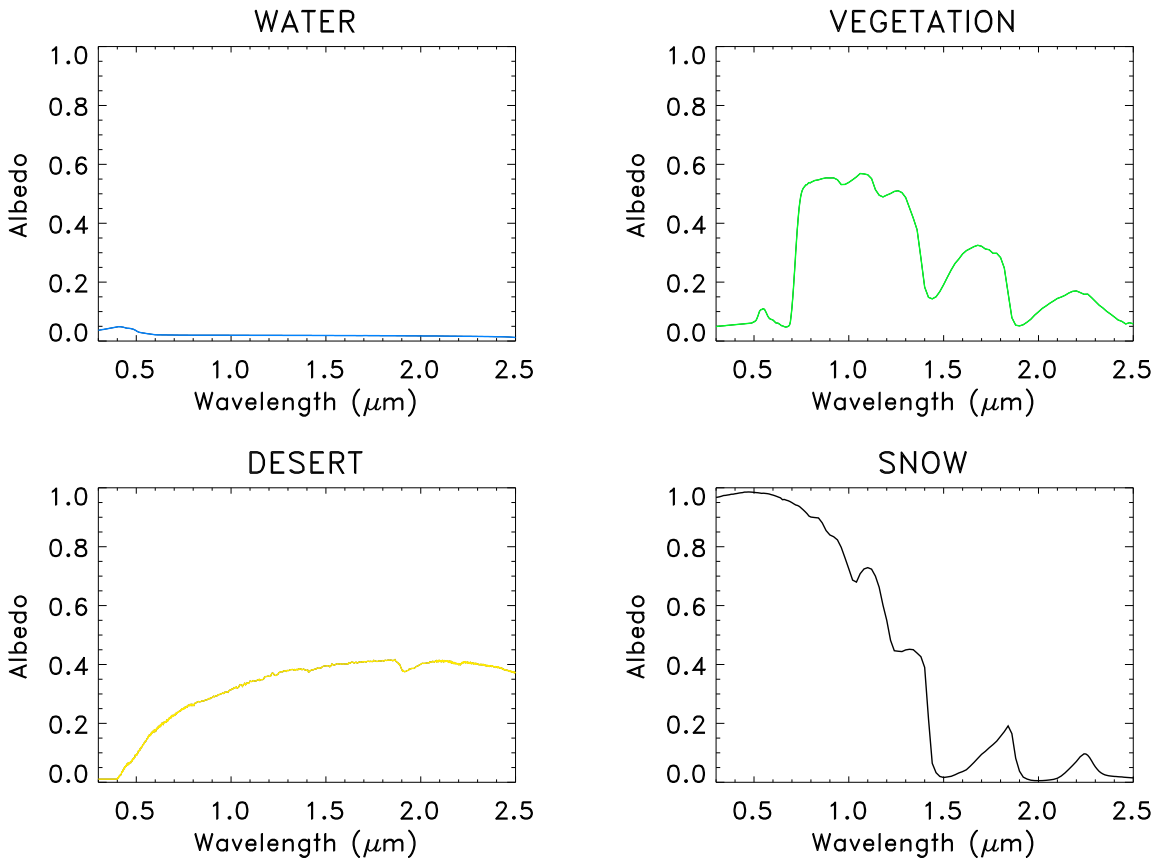


Fig. 2.— Spectral reflectance of water, vegetation, desert, and snow. Data taken from the ASTER Spectral Library and the USGS Digital Spectral Library.

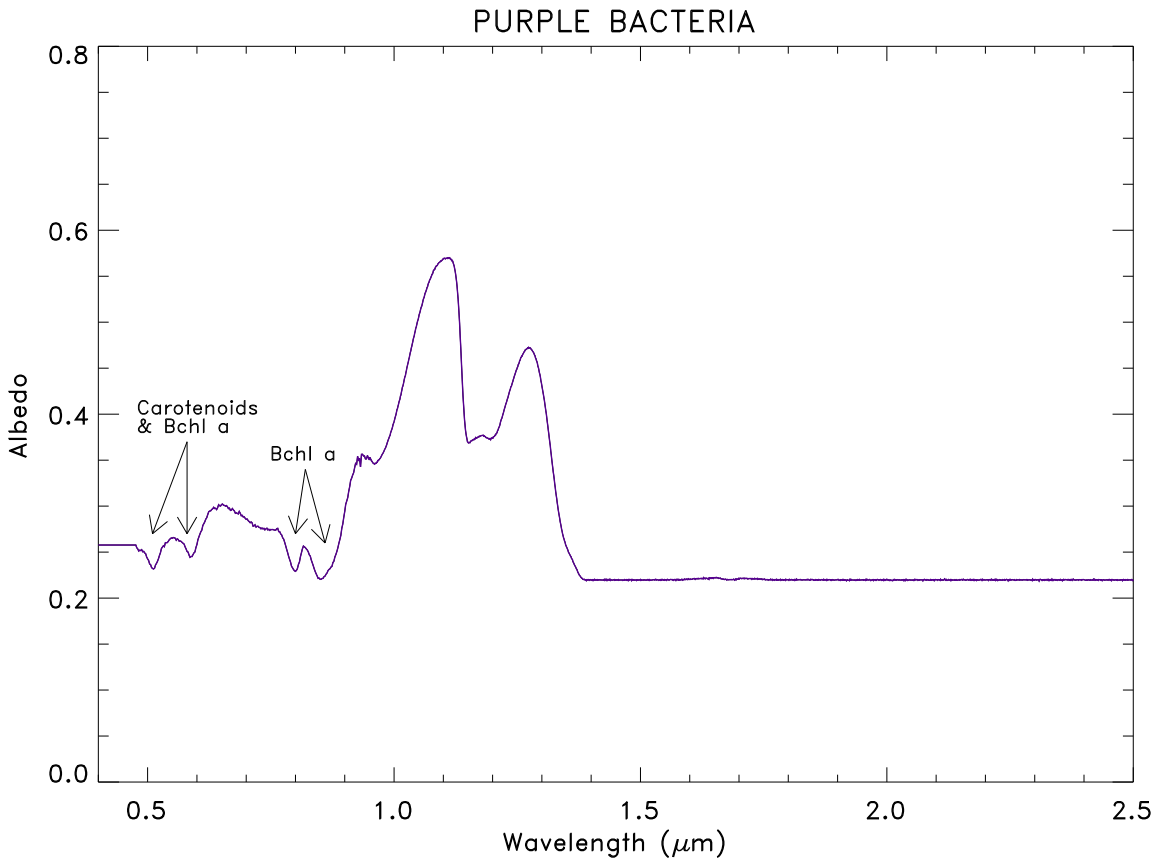


Fig. 3.— Wavelength-dependent albedo obtained for purple bacteria in the VIS-NIR spectral range where major absorption features of carotenoids and *bacteriochlorophyll a* are labeled .

Table 1: Strength of the purple bacteria signal as a function of bacteria percentage in oceans.

Bact. in Water	No Clouds	With Clouds
10%	0.0295	0.0088
20%	0.0400	0.0140
30%	0.0505	0.0193
40%	0.0610	0.0245
50%	0.0715	0.0298

Note. — Slope between the intensity in the 0.745-0.770 μm and the 1.010-1.034 μm range.

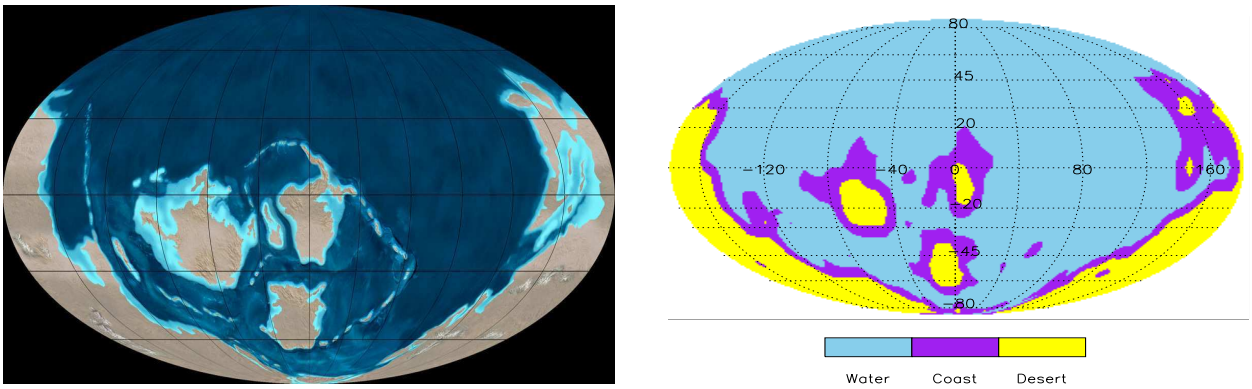


Fig. 4.— Left: A map of the Earth's continental distribution during the Late Cambrian (500 Ma ago). Image credit, Ron Blakey. Right: Same as in left panel but here oceans, continents and coastal zones are indicated in blue, yellow and purple, respectively. Data are plotted with a geographical resolution of 64x32 grid cells (longitude by latitude), the same that our models use. Coastal areas constitute 14% of the total grid cells when using this continental distribution and geographic resolution. In our simulations the 00:00 hours UT, correspond to the subsolar point crossing the image center.

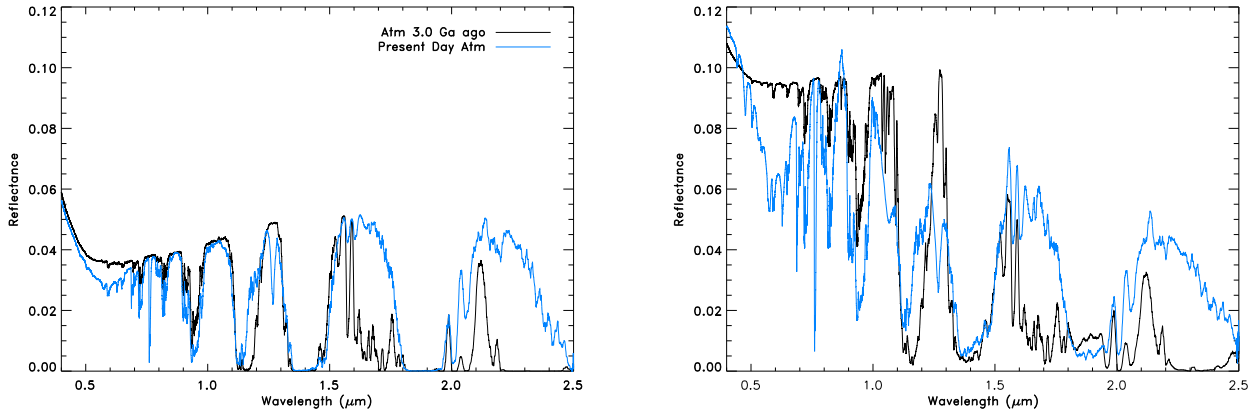


Fig. 5.— Visible and near-infrared disk-averaged spectra of a planet with a continental distribution of the Earth 500 Ma ago, with an atmospheric composition similar to that of the Earth 3.0 Ga ago (black), and with present-day composition (blue). Here, continents are totally desert and we have considered both, a cloud-free atmosphere (left), and a cloudy atmosphere (right). We have assumed that clouds cover 50% of the surface. The spectra have been smoothed with a 100 point running mean for display purposes.

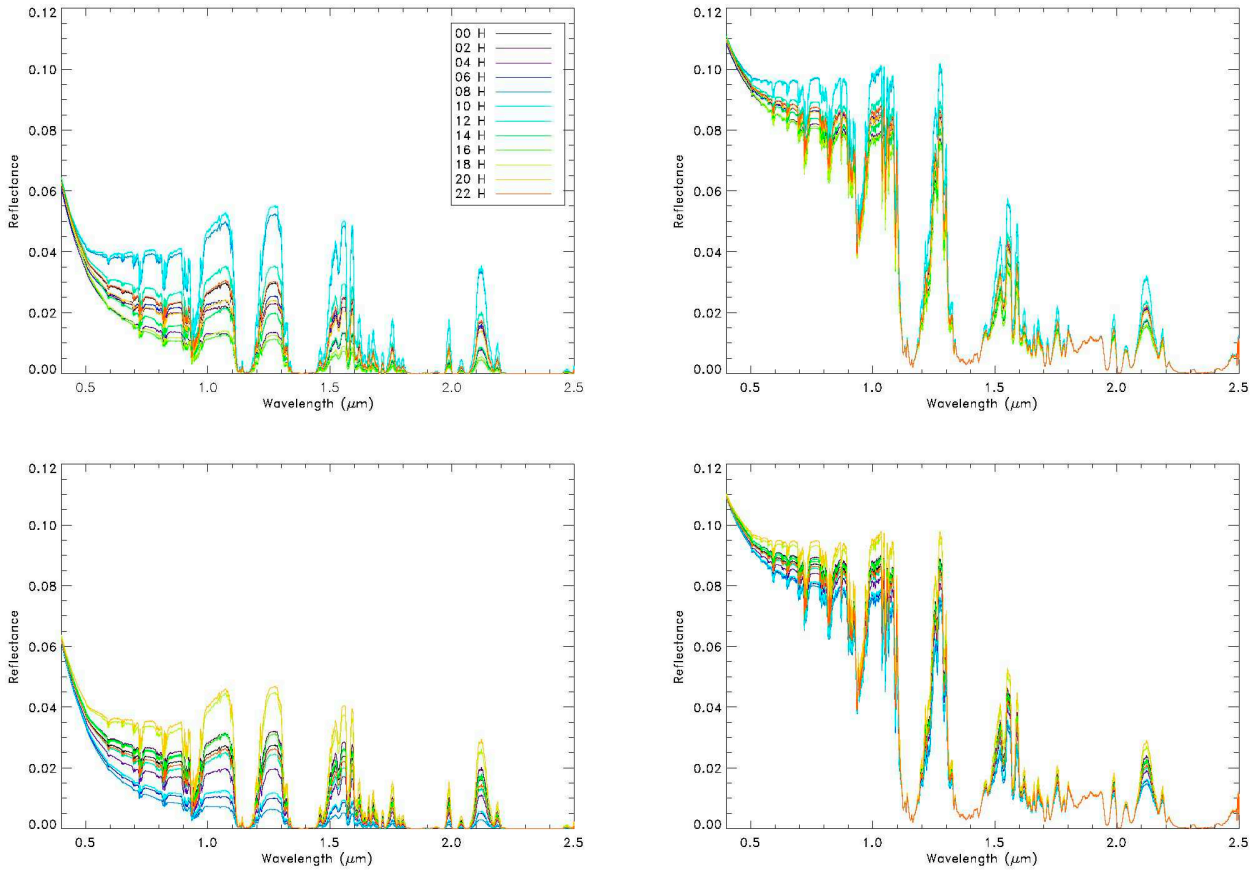


Fig. 6.— Visible and near-infrared Earth's reflectance spectra 3.0 Ga ago, taken as π times the disk-integrated radiance divided by the solar flux, over the course of a day. Continents are totally desert and coastal points that are closest to continent are totally populated by purple bacteria, and coastal points that are closest to oceans are a mixture of purple bacteria, 10%, and water, 90%. Left panels show a cloud-free atmosphere and the right panels show a cloudy atmosphere. We have assumed that clouds cover 50% of the surface and continental distribution corresponds to that of the Earth 500Ma ago (top panels) and that of present Earth (bottom panels). The spectra have been smoothed with a 100 point running mean for display purposes.

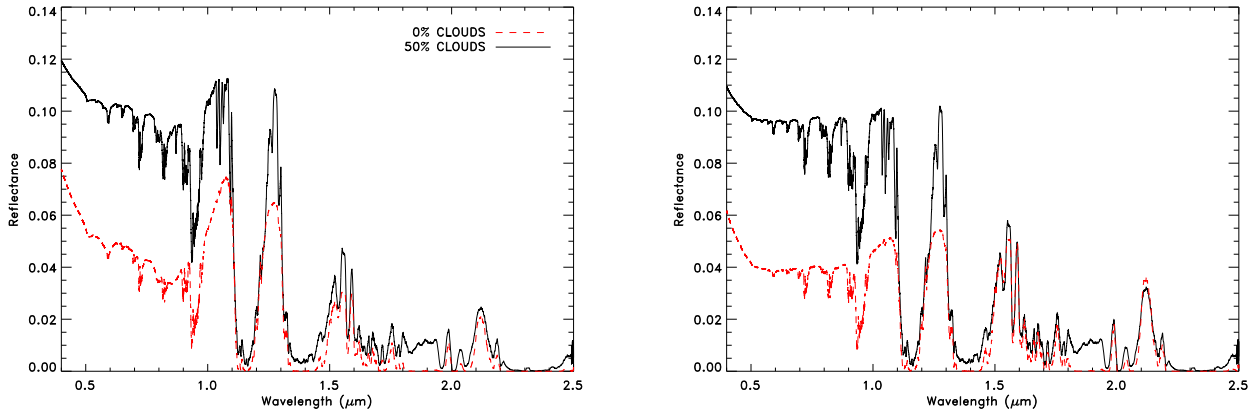


Fig. 7.— Visible and near-infrared disk-integrated spectra of the early Earth for a cloud-free atmosphere (red dashed lines) and a 50% cloudy atmosphere (black solid lines). In the left panel, continents are totally covered by mats of purple bacteria and oceans are a mixture of water and purple bacteria (90% and 10%, respectively). The same is shown in the right figure but here continents are bare deserts.

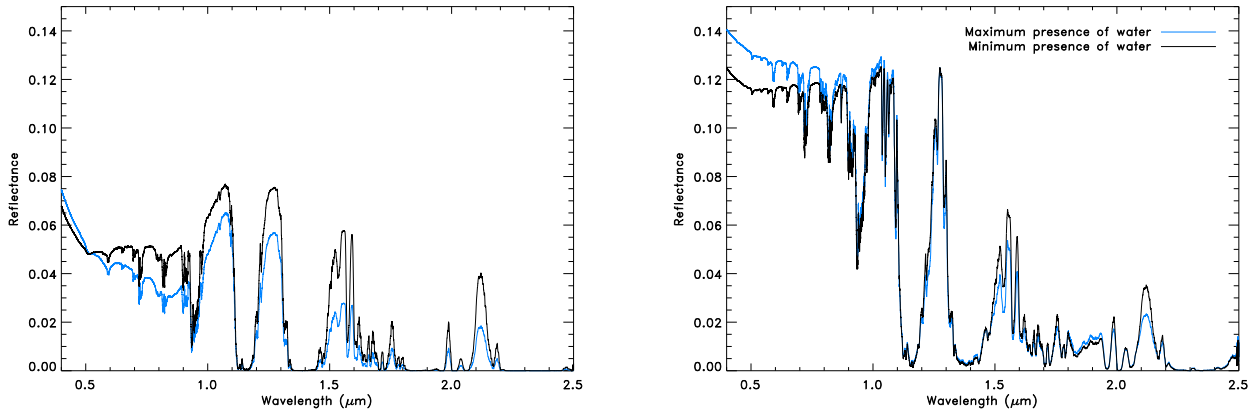


Fig. 8.— Disk-averaged spectra of Earth for cloud-free (left) and a cloudy atmosphere (right). Here the continental and cloud distribution is that of present-day Earth and the atmospheric composition corresponds to that of the early Earth (3.0 Ga ago). Continents are assumed to be deserts, coastal zones are completely populated with purple bacteria, and oceans are a mixture of water and purple bacteria according to the present-day chlorophyll a distribution. Blue lines represent when oceans dominate de field of view and black lines when continents do.

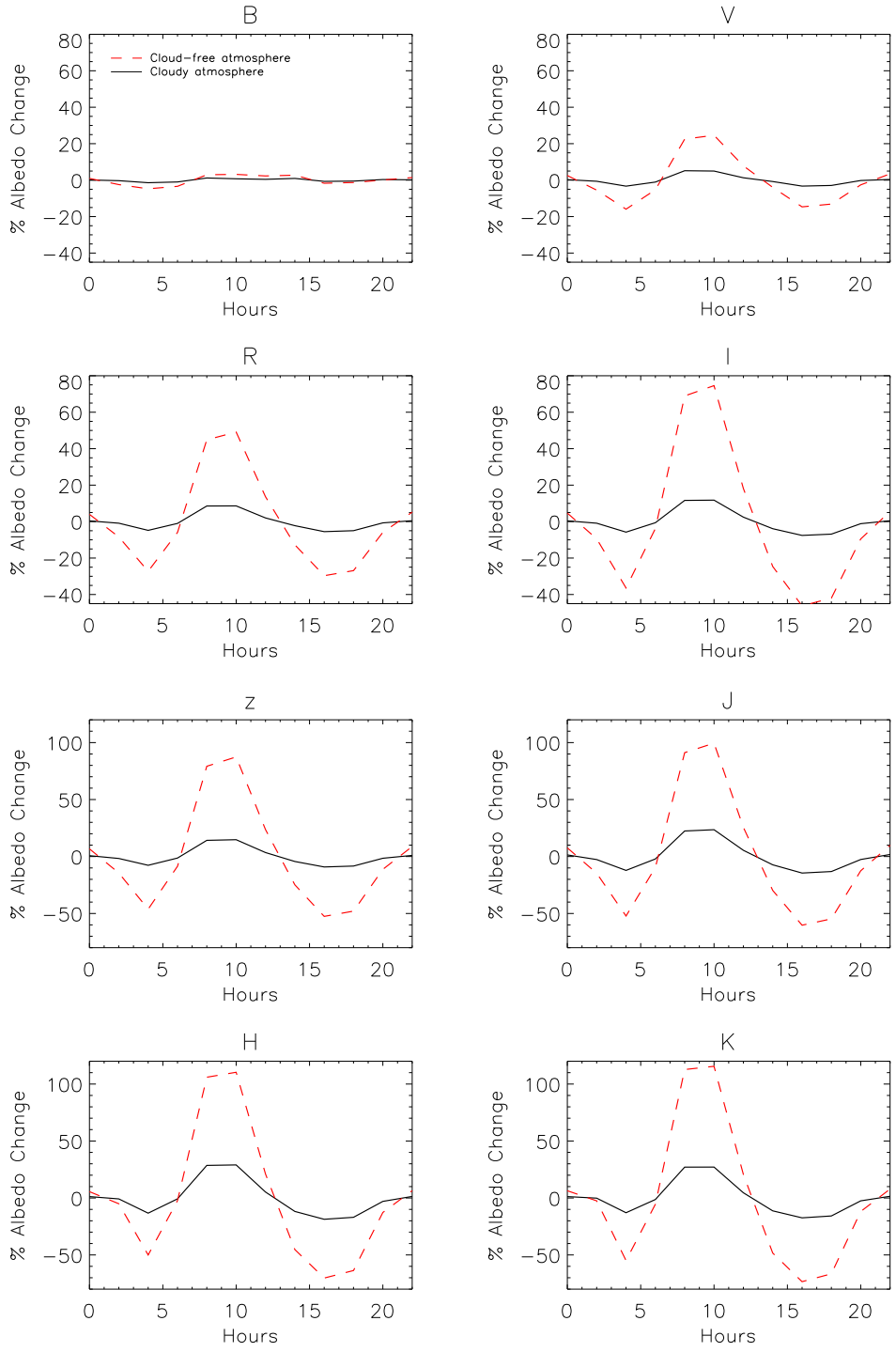


Fig. 9.— Daily variations of the light reflected by the early Earth for a cloud-free (red lines) and for a cloudy atmosphere (black lines). Cloud cover is assumed to be 50%. The continental distribution is that of the Earth 500Ma ago. Continents are completely covered by deserts, coastal land areas are covered by purple bacteria mats, and oceanic coastal areas are a mixture of 10% bacteria and 90% water.

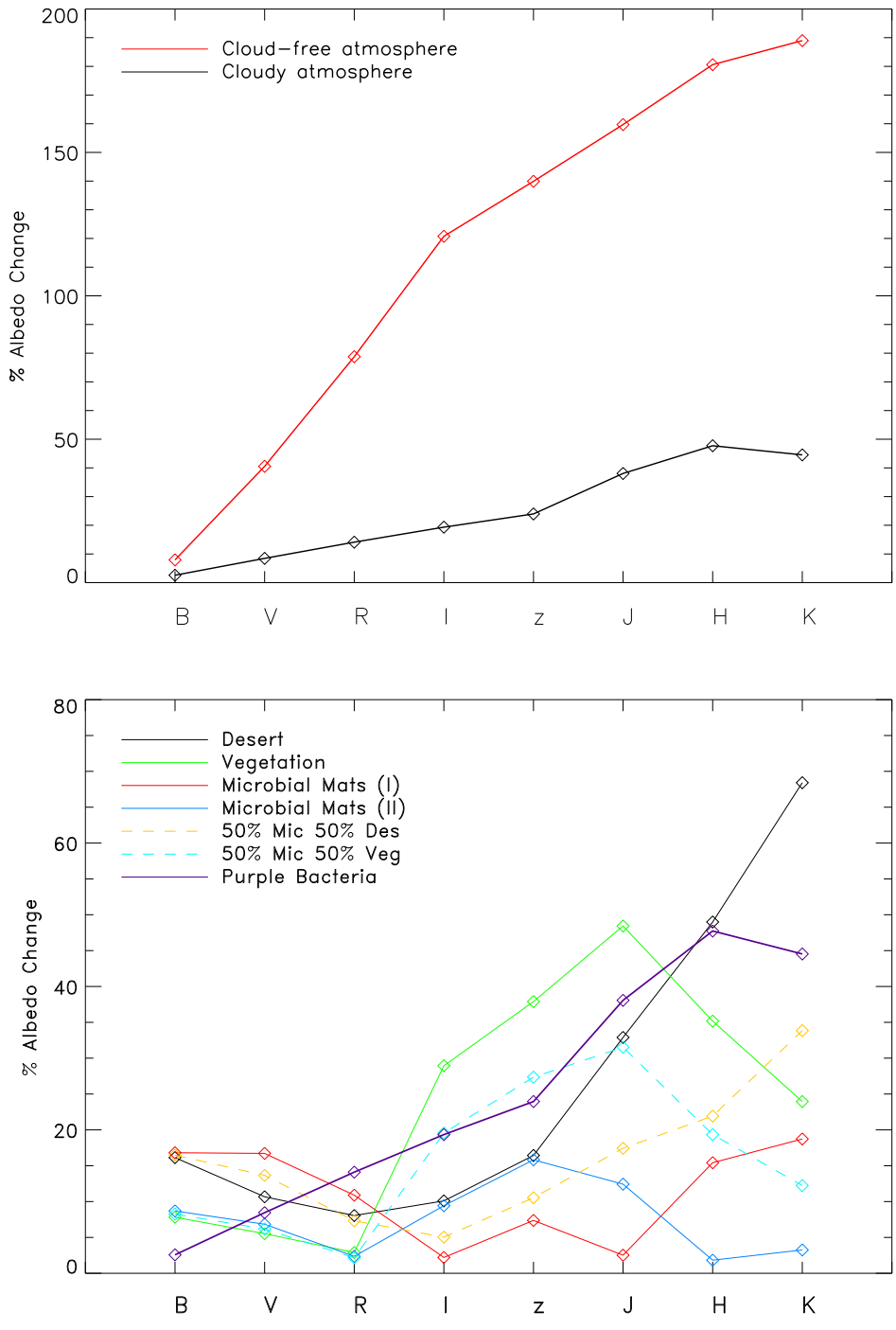


Fig. 10.— Top: Amplitude of the albedo variability of the early Earth as a function of the standard photometric filters. Continents are covered by deserts and coasts are a mixture of purple bacteria and water. Black represents a cloudy atmosphere and red a cloud-free atmosphere. Bottom: Figure 6 published in Sanromá et al. (2013) including the amplitude variability of the cloudy case shown in the top of this Figure.